Biosensors and Bioelectronics 41 (2013) 698–703

Contents lists available at SciVerse ScienceDirect

Biosensors and Bioelectronics

journal homepage: www.elsevier.com/locate/bios

# Carbon nanotubes-nanoflake-like $SnS_2$ nanocomposite for direct electrochemistry of glucose oxidase and glucose sensing

Juan Li [1], Zhanjun Yang [1,*], Yan Tang, Yongcai Zhang, Xiaoya Hu *

*College of Chemistry and Chemical Engineering, Yangzhou University, Jiangsu Key Laboratory of Environmental Engineering and Monitoring, Yangzhou 225002, PR China*

ARTICLE INFO

*Article history:*
Received 28 June 2012
Received in revised form
24 September 2012
Accepted 25 September 2012
Available online 4 October 2012

*Keywords:*
Nanoflake-like $SnS_2$
Carbon nanotubes
Glucose oxidase
Direct electrochemistry
Glucose
Biosensor

ABSTRACT

Multi-walled carbon nanotubes (MWCNTs)–nanoflake-like $SnS_2$ nanocomposite were designed for immobilization of glucose oxidase (GOx). The direct electrochemistry of GOx and glucose sensing at MWCNTs–$SnS_2$ modified glassy carbon electrode were studied. Compared with single MWCNTs or $SnS_2$, the MWCNTs–$SnS_2$ film has larger surface area and provides a more favorable microenvironment for facilitating the electron transfer between enzyme and electrode surface. The properties of GOx/MWCNTs–$SnS_2$ were examined by scanning electron microscopy, UV–vis spectroscopy, Fourier transform infrared spectroscopy and cyclic voltammetry. The immobilized enzyme on MWCNTs–$SnS_2$ composite film retained its native structure and bioactivity and showed a surface controlled, reversible two-proton and two-electron transfer reaction with a apparent electron transfer rate constant of $3.96\ s^{-1}$. The constructed glucose biosensor exhibits wider linear range from $2.0\times10^{-5}$ M to $1.95\times10^{-3}$ M, much lower detection limit of $4.0\times10^{-6}$ M at signal-to-noise of 3 and higher sensitivity of $21.65\ mA\ M^{-1}\ cm^{-2}$ than our previous nanoflake-like $SnS_2$-based glucose sensor. The proposed biosensor has excellent selectivity, good reproducibility, and acceptable operational stability and can be successfully applied in the reagentless glucose sensing at −0.43 V. This MWCNTs–$SnS_2$ composite provides a new avenue for immobilizing proteins and fabricating excellent biosensors.



## 1. Introduction

$SnS_2$ is an n-type semiconductor with a bandgap of 2.18–2.44 eV (Deshpande et al., 2007; Panda et al., 2007), and has good stability in acid and neutral aqueous solutions as well as certain oxidative and thermal stability in air, which makes it a promising visible light-sensitive photocatalyst (Yang et al., 2009). Besides, owing to its intriguing electrical, optical and gas sensing properties, $SnS_2$ has been employed as a candidate material in solar cells and opto-electronic devices (Deshpande et al., 2007; Panda et al., 2007), electrode for lithium-ion batteries (Kim et al., 2007; Seo et al., 2008), pigment and gas sensor (Shi et al., 2006). However, $SnS_2$ have been seldom reported to immobilize proteins for electrochemical biosensing. In our previous works, nanoflake-like $SnS_2$ was for the first time employed for direct electron transfer (DET) of proteins and glucose biosensing (Yang et al., 2011).

DET between biomolecules (enzymes or proteins) and electrode surface in biological systems is a very important phenomenon for developing biosensor, biofuel cells and biomedical devices without mediator (Lu et al., 2007; Wen et al., 2007; Wu et al., 2007; Willner and Katz, 2000). Unfortunately, the redox center in biomolecules is usually seated deeply in cavity of enzyme molecules, which makes it hard to realize DET of enzyme at conventional electrode (Meng et al., 2009). Recently, great efforts have been made to develop novel reagentless biosensor and biomedical devices based on DET of enzyme by immobilizing it on nanomaterials modified electrode (Liu and Ju, 2003; Nadzhafova et al., 2007; Bao et al., 2008; Jia et al., 2008; Pingarron et al., 2008; Kang et al., 2009; Shan et al., 2010a, b; Tang, et al., 2010; Yang et al., 2012; Yin et al., 2011; Zhang et al., 2012). Carbon nanotubes (CNTs), since discovered in 1991 (Iijima, 1991), have attracted considerable research interest in electrochemical biosensing fields due to their unique physical and electronic properties such as high electronic conductivity, high surface/volume ratio and unique ability to promote electron transfer (Zhao and Ju (2006); Chu et al., 2010). CNTs and CNTs-based composites have been used to modify electrode for DET of glucose oxidase (GOx) and glucose biosensing (Liu et al., 2005; Deng et al., 2008, 2009; Dai et al., 2009; Li et al., 2009; Wang et al., 2011).

As an ideal mode enzyme used in the electrochemical biosensors, GOx has been extensively applied to monitor the blood glucose levels in diabetics due to its catalytic ability to oxidize glucose (Vamvakai et al., 2006); Salimi et al., 2007; Shan et al., 2010a, b; Xu et al., 2010). In this work, nanoflake-like $SnS_2$ was

* Corresponding authors. Tel./fax: +86 514 87972034.
*E-mail addresses:* zjyang@yzu.edu.cn (Z. Yang), xyhu@yzu.edu.cn (X. Hu).
[1] The first two authors contributed equally to this work.

0956-5663/$ - see front matter © 2012 Elsevier B.V. All rights reserved.
http://dx.doi.org/10.1016/j.bios.2012.09.059

mixed with multi-walled carbon nanotubes (MWCNTs), and then the resulted MWCNTs–$SnS_2$ was for the first time employed for fabricating the enzyme biosensor based on DET of GOx. The MWCNTs–$SnS_2$ film was favorable for enhancing electron transfer between the biomolecules and the electrode surface. A pair of well-defined redox peaks of GOx was obtained at GOx/MWCNTs–$SnS_2$/nafion modified electrode. UV–vis and Fourier transform infrared (FTIR) spectrum displayed that the MWCNTs–$SnS_2$ film provided a favorable microenvironment for GOx to retain its native structure and bioactivity. The constructed biosensor showed good reproducibility and excellent selectivity and was successfully applied in the reagentless glucose detection. Moreover, the CNTs–$SnS_2$ composite can provide a promising alternative for electrochemical biosensing.

## 2. Materials and methods

### 2.1. Materials and reagents

GOx (EC 1.1.3.4, 108 U $mg^{-1}$, from *Aspergillus niger*) was supplied by Amresco. D-(+)-Glucose and Nafion were purchased from Sigma-Aldrich. Tin (II) chloride dehydrate ($SnCl_2 \cdot 2\,H_2O$) and sulfur (S) were purchased from Sinopharm Chemical Reagent Co., Ltd. MWCNTs ($\geq$98% purity, 60–100 nm diameter and 1–2 μm length) were bought from Shenzhen Nanoport Co. Ltd. A stock solution of D-glucose was prepared and allowed to mutarotate at room temperature for 24 h before measurements. Phosphate buffer solution (PBS) was a mixture of 0.1 M $Na_2HPO_4$ and $NaH_2PO_4$ and its pH was adjusted with $H_3PO_4$ or NaOH solutions. All other chemicals and reagents are of analytical grade and were prepared using distilled water.

### 2.2. Apparatus

Electrochemical measurements were carried out on a CHI 852C electrochemical workstation (Co., CHI, USA). All experiments were performed with a three-electrode system using a glassy carbon electrode (GCE, $\Phi$=3 mm) as the working electrode, a platinum wire as the auxiliary electrode and a saturated calomel electrode (SCE) as reference electrode. The cyclic voltammetric experiments were carried out at a scan rate of 50 mV $s^{-1}$ in an electrochemical cell filled with 5.0 ml of PBS. All pH measurements were made with S-25 digital pH-meter with glass combination electrode.

Scanning electron micrographs (SEM) were obtained with a Hitachi S-4800 scanning electron microscope (Japan) at an acceleration voltage of 15 kV. Fourier transform infrared (FTIR) spectra were measured with a Tensor 27 spectrophotometer (Bruker Co., Germany). UV–vis spectra were recorded by UV-2550 spectrophotometer (Shimadzu Co., Japan).

### 2.3. Preparation of MWCNTs–$SnS_2$ and enzyme electrodes

Nanoflake-like $SnS_2$ was simply synthesized according to the previous method (Zhang et al., 2010). MWCNTs were firstly dispersed in 30% nitric acid and then refluxed for 24 h at 140 °C. The resulting suspension was centrifuged, and the sediment was rinsed with water until the pH reached about 7.0 and dried in air at 60 °C. Subsequently, 0.6 mg of carboxylated MWCNTs and 0.2 mg of yellow nanoflake-like $SnS_2$ were dispersed together in 1.0 ml distilled water with ultrasonication for 0.5 h and then the suspension of MWCNTs–$SnS_2$ was obtained for the following use.

The GCE was firstly polished successively with 0.03 and 0.05 μm alumina slurry (Buhler) followed by rinsing thoroughly with distilled water, and then sonicated in 1:1 nitric acid, acetone and distilled water, respectively. After being dried in air, the pretreated GCE was modified by dropping 5.0 μl of the suspension of MWCNTs–$SnS_2$ on the surface and dried in silica gel desiccators. 5.0 μl of 5 mg $ml^{-1}$ GOx solution was then dropped on the MWCNTs–$SnS_2$ modified GCE and dried in silica gel desiccators. After 5.0 μl of 0.5% Nafion solution was dropped on the GOx/MWCNTs–$SnS_2$ modified electrode surface, the GOx/MWCNTs–$SnS_2$/Nafion modified electrode was finally obtained. The resulted electrode was rinsed thoroughly with distilled water to wash away the loosely adsorbed enzyme molecules. When not in use, the fabricated electrode was stored in 0.1 M, pH 7.0 PBS at 4 °C in a refrigerator.

## 3. Results and discussion

### 3.1. Characterizations of $SnS_2$, MWCNTs–$SnS_2$, GOx and GOx/MWCNTs–$SnS_2$

The synthesized nanoflake-like $SnS_2$ was firstly mixed with MWCNTs and subsequently employed to immobilize GOx. The SEM image of the synthesized $SnS_2$ is shown in Fig. 1a, which exhibits an anisotropic and uniform flake-like morphology with about 40 nm flake thickness. As seen from the SEM image of MWCNTs–$SnS_2$ (Fig. 1b), the surface of the synthesized $SnS_2$ have been wrapped by MWCNTs, forming the MWCNTs–$SnS_2$ nanocomposite. Fig. 1c shows the SEM of GOx/MWCNTs–$SnS_2$, which displays obviously different surface morphology from MWCNTs–$SnS_2$, suggesting that GOx biomolecules have been successfully immobilized in the MWCNTs–$SnS_2$ nanocomposite film.

UV–visible spectroscopy was used to study the possible conformational change of GOx in MWCNTs–$SnS_2$ film. The UV–visible absorption spectra of MWCNTs–$SnS_2$, GOx and GOx/MWCNTs–$SnS_2$ are shown in Fig. 2A. MWCNTs–$SnS_2$ showed no obvious absorption peaks in the range of 200–600 nm. For the native GOx, the absorption peak at 278 nm was ascribed to the characteristic of polypeptide chains, and the two weak peaks at 382 and 456 nm were attributed to the oxidized form of flavin group in protein

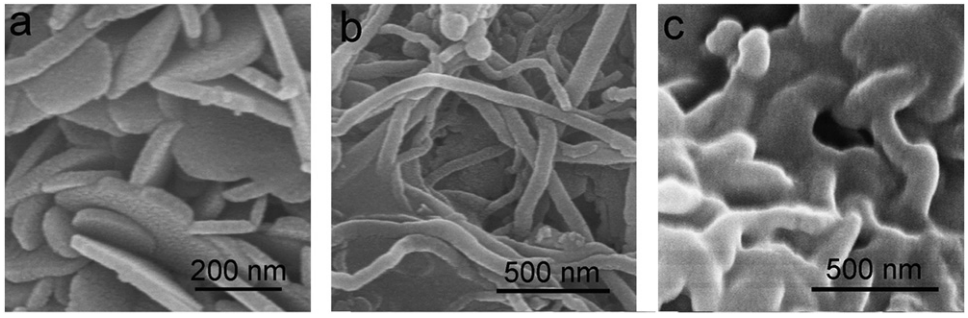


**Fig. 1.** SEM images of nanoflake-like $SnS_2$ (a), MWCNTs–$SnS_2$ (b) and GOx/MWCNTs–$SnS_2$ (c).

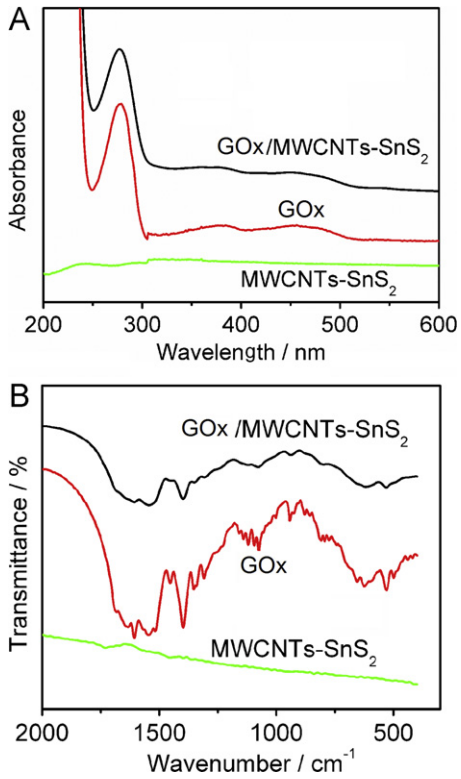


**Fig. 2.** UV–vis absorption spectra (A) and FTIR spectra of (B) of MWCNTs–$SnS_2$, GOx and GOx/MWCNTs–$SnS_2$.

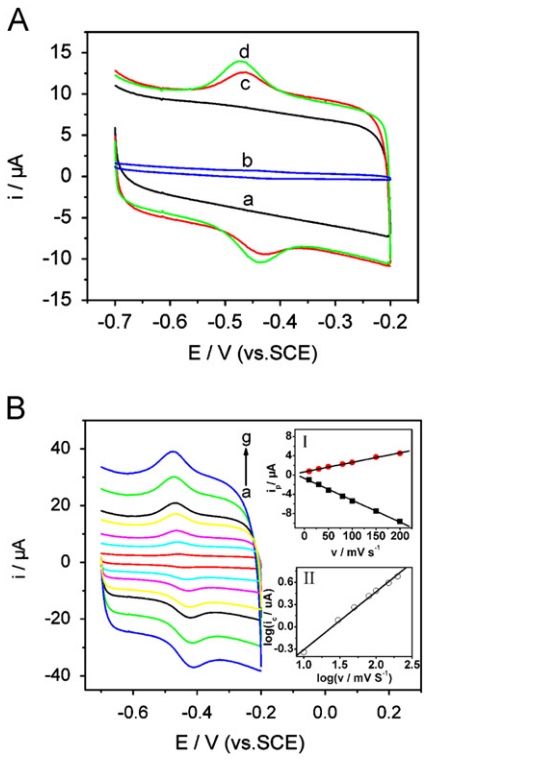


**Fig. 3.** Cyclic voltammograms for (a–d) $SnS_2$/Nafion/GCE, GOx/Nafion/GCE, GOx/MWCNTs/Nafion/GCE and GOx/MWCNTs–$SnS_2$/Nafion/GCE in 0.1 M, pH 6.0 $N_2$-saturated PBS at a scan rate of 50 mV $s^{-1}$ (A) and cyclic voltammograms of the GOx/MWCNTs–$SnS_2$/Nafion/GCE in 0.1 M, pH 6.0 $N_2$-saturated PBS at 10, 30, 50, 80, 100, 150 and 200 mV $s^{-1}$ (from a to g). Inset (I): plots of anodic and cathodic peak currents vs. scan rates; Inset (II): plot of logarithm of $i_{pc}$ vs. logarithm of $v^{-1}$.

structure (Liu and Hu, 2007). The position and shape of absorption bands for GOx/MWCNTs–$SnS_2$ were almost the same as those of pure GOx, indicating that the GOx immobilized in MWCNTs–$SnS_2$ nanocomposite film indeed maintained its native structure (Shan et al., 2010a, b).

FTIR spectroscopy was further used to examine the existing state of the immobilized GOx. Fig. 2B shows the FTIR spectra of the MWCNTs–$SnS_2$, native GOx and GOx immobilized in MWCNTs–$SnS_2$ nanocomposite. In the case of the MWCNTs–$SnS_2$, no obvious absorption peak was observed. The FTIR spectrum of native GOx displayed two characteristic peaks at 1612 and 1550 $cm^{-1}$, respectively, which were ascribed to amide I and II bands of enzyme. The two absorption peaks were also observed in the FTIR spectrum of GOx/MWCNTs–$SnS_2$ at 1608 $cm^{-1}$ (amide I band) and 1537 $cm^{-1}$ (amide II band), indicating that GOx has been successfully immobilized in the MWCNTs–$SnS_2$ nanocomposite film (Shi et al., 2003). A small difference was found in the absorption peaks position of the amide I and II bands between native GOx and GOx immobilized in nanocomposite film, which might result from the intermolecular interaction between enzyme and MWCNTs–$SnS_2$ film (Fan et al., 2007).

### 3.2. Direct electrochemistry of GOx/MWCNTs–$SnS_2$/Nafion/GCE

As a part of the GOx molecule, FAD is known to undergo the redox reaction where two protons and two electrons are released or taken up (Ianniello et al., 1982; Liu and Ju, 2003). DET between GOx and substrate can be observed from the electrochemical response under proper conditions, which are further used to fabricate electrochemical biosensor (Nadzhafova et al., 2007; Deng et al., 2009; Kang et al., 2009; Shan et al., 2010a, b). Fig. 3A shows the cyclic voltammograms of different modified GCE in 0.1 M $N_2$ saturated PBS at a scan rate of 50 mV $s^{-1}$. No peaks were observed for MWCNTs–$SnS_2$/Nafion/GCE (curve a). The high background current of MWCNTs–$SnS_2$/GCE was attributed to the larger surface area of MWCNT wrapped $SnS_2$ (Kang et al., 2009). Compared to the GOx/Nafion/GCE (curve b), GOx/MWCNTs/Nafion/GCE (curve c) showed a pair of distinct and well-defined redox peaks. However, after immobilizing GOx in MWCNTs–$SnS_2$ nanocomposite film, GOx/MWCNTs–$SnS_2$/Nafion/GCE displayed a pair of more distinct and better-defined redox peaks at −0.436 V and −0.472 V (curve d). Accordingly, the MWCNTs–$SnS_2$ is considered to enable more effective electrical contact between redox-active centers of enzyme and electrode surface, leading to the enhanced direct electrochemistry of GOx (Willner et al., 2006). The peak potential separation was 36 mV, which is much smaller than that of 80 mV at GOx/graphene–chitosan modified GCE (Kang et al., 2009), indicating the faster DET between the redox-active site of GOx (the cofactor FAD) and GCE without the help of electron transfer mediator (Deng et al., 2009). The number of electron transferred in the electrochemical process was 2 ($n \approx 1.6$ based on the formula of $59/n$ at 25 °C).

Fig. 3B shows the effect of the scan rate on the cyclic voltammetric performance at the GOx/MWCNTs–$SnS_2$/Nafion modified GCE. With the increase of the scan rate, the redox potentials of GOx shifted slightly. The anodic current ($I_{pa}$) and cathodic peak current ($I_{pc}$) linearly increased with the increasing scan rate from 10 to 200 mV $s^{-1}$ (inset I of Fig. 3B) and the $I_{pa}/I_{pc}$ ratio is approximately equal to 1, indicating that the redox reaction of GOx in MWCNTs–$SnS_2$ modified GCE was a quasi-reversible surface-controlled process. The logarithm plot of cathodic peak current versus logarithm of the san rate showed a linear relationship (inset II of Fig. 3B), which was close to the theoretical slope for thin layer electrochemical behavior (Shan et al., 2010a, b). According to Laviron's equation (Laviron, 1979), the charge-transfer coefficient and the apparent electron transfer rate constant ($k_s$) for the proposed electrode were calculated to be

0.5 and 3.96 $s^{-1}$, respectively. The obtained value of $k_s$ was larger than those of 1.56 $s^{-1}$ at boron-doped carbon nanotubes (Deng et al., 2008), 1.7 $s^{-1}$ at multi-walled carbon nanotubes (Guiseppi-Elie et al., 2002), and 2.83 $s^{-1}$ at graphene–chitosan modified GCE (Kang et al., 2009). This result further confirms that nanoflake-like $SnS_2$ facilitates the fast electron transfer between the redox-active site of enzyme and the surface of electrode.

The surface coverage ($\Gamma^*$) of the electroactive GOx on surface of the MWCNTs–$SnS_2$ modified electrode can be obtained according to the formulation $\Gamma^*=Q/nFA$, where $Q$ is the charge consumed in the reaction, $n$ is the number of electrons transferred, $F$ is the Faraday constant, and $A$ is the electrode area. The surface coverage was then calculated to be $2.75\times10^{-11}$ mol $cm^{-2}$ using the charge integration of cathodic peak in CVs at 50 mV $s^{-1}$, which was larger than those of $1.60\times10^{-11}$ mol $cm^{-2}$ at GOx/$SnS_2$/Nafion/GCE (Yang et al., 2011), $9.8\times10^{-12}$ mol $cm^{-2}$ at GOx/Au nanoparticles/carbon paste electrode (Liu and Ju, 2003), $7.82\times10^{-12}$ mol $cm^{-2}$ at GOx/Au-dihexadecyl phosphate modified electrode (Wu and Hu, 2007) and $2.86\times10^{-12}$ mol $cm^{-2}$ at bare GCE (Zhang et al., 2007), indicating the saturated absorption of the multilayer GOx in the MWCNTs–$SnS_2$ composite film. The influence of the pH value on the electrochemical behavior of GOx in MWCNTs–$SnS_2$ film was investigated. With the increase of the solution pH from 4.0 to 8.0, both the cathodic and anodic peak potentials shifted negatively. The redox potentials of GOx/MWCNTs–$SnS_2$/Nafion/GCE changed linearly as a function of the solution pH with a slope of $-54.1$ mV $pH^{-1}$ during the reduction process. This slope was close to the theoretical value of $-58.6$ mV $pH^{-1}$ (Deng et al., 2009), indicating two protons and two electrons participating in the electron transfer process (As the number of electron transferred in the electrochemical process was 2).

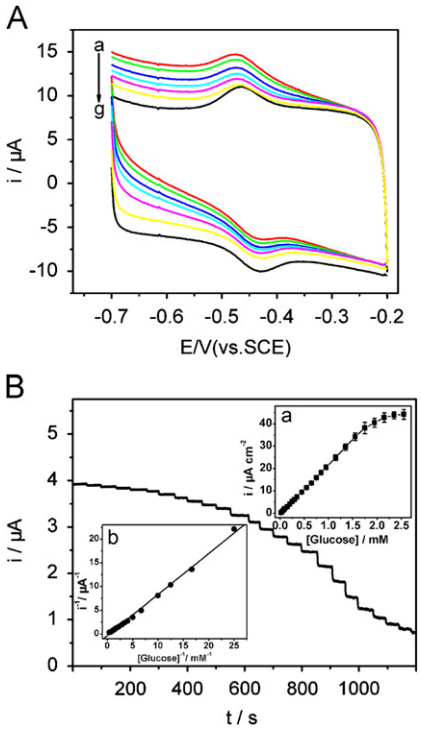


**Fig. 4.** Cyclic voltammograms of the GOx/MWCNTs–$SnS_2$/Nafion/GCE (A) in 0.1 M pH 6.0 air-saturated PBS (a), air-saturated PBS including 0.1 mM, 0.3 mM, 0.5 mM, 0.8 mM, 1.0 mM glucose (b–f) and $N_2$-saturated PBS (g) at a scan rate of 50 mV $s^{-1}$; Typical steady-state response of the GOx/MWCNTs–$SnS_2$/Nafion/GCE (B) on successive addition of glucose into 0.1 M pH 6.0 air-saturated PBS at the applied potential of $-0.43$ V. Inset of (a): calibration curve of the GOx/MWCNTs–$SnS_2$/Nafion/GCE for glucose; Inset of (b): plot of $j^{-1}$ vs. $[Glucose]^{-1}$.

### 3.3. Performance of the proposed glucose biosensor

In air-saturated PBS, the cyclic voltammogram of GOx/MWCNTs–$SnS_2$/Nafion/GCE showed a great increase in reduction peak current and a simultaneous decrease in oxidation current (curve a in Fig. 4A). This result demonstrated that GOx ($FADH_2$) exerted an obvious electrocatalytic process toward the reduction of dissolved oxygen according to the following equations (Liu and Ju, 2003):

$$GOx(FAD)+2e^-+2H^+ \leftrightarrow GOx(FADH_2) \quad (1)$$

$$GOx(FADH_2)+O_2 \rightarrow GOx(FAD)+H_2O_2 \quad (2)$$

In the presence of oxygen, regenerated GOx (FAD) resulted in the increase of the reduction peak current of FAD. When glucose was added into this system, it restrained the electrocatalytic reaction due to the enzyme-catalyzed reaction, which reduced the concentration of GOx (FAD) as shown in the following equation:

$$Glucose+GOx(FAD)+O_2 \rightarrow Gluconolactone+GOx(FADH_2) \quad (3)$$

Thus the reduction peak current of GOx decreased with the increase of glucose concentration (curves b–f in Fig. 4A). The glucose biosensor was therefore proposed based on the decease. Fig. 4B showed the typical amperometric response curves at GOx/MWCNTs–$SnS_2$/Nafion modified GCE on successive injection of glucose to the air-saturated stirring PBS (the optimal potential and pH value for the amperometric detection of glucose were chosen as –0.43 V and 6.0, respectively). The GOx/MWCNTs–$SnS_2$/Nafion/GCE achieved 95% of the steady-state current within 7 s. The response increased linearly with the increase of glucose concentration ranging from $2.0\times10^{-5}$ to $1.95\times10^{-3}$ M with a low detection limit of $4.0\times10^{-6}$ M at signal-to-noise of 3 (Inset a of Fig. 4B). The sensitivity of GOx/MWCNTs–$SnS_2$/Nafion/GCE was calculated to be 21.65 mA $M^{-1}$ $cm^{-2}$. The comparison of these analytical performances to those recently reported in the literatures involving in the glucose biosensor based on DET is shown in Table 1. The results demonstrated that the GOx/MWCNTs–$SnS_2$/Nafion/GCE showed obvious predominance in sensitivity and detection limit compared with the GOx/$SnS_2$/Nafion/GCE and GOx/CNTs or GOx/CNTs composite modified electrodes.

The apparent Michaelis–Menten constant ($K_M^{app}$) was calculated to be 2.71 mM for the glucose biosensor according to the slope and the intercept of the plot of the reciprocals of the steady-state current vs. glucose concentration (Inset b of Fig. 4B). The $K_M^{app}$ values was much smaller than those of 4.4, 11.6 mM and 37.6 mM for immobilized GOx (Zheng et al., 2002; Uang and Chou, 2003; Kang et al., 2009), indicating that the GOx immobilized on MWCNTs–$SnS_2$ showed high affinity towards glucose.

### 3.4. Reproducibility and stability of the glucose biosensor

The reproducibility of the proposed biosensor was investigated by successively detecting 0.1 mM glucose for 5 times, the relative standard deviation (RSD) was 2.7%, indicating a good reproducibility. After 20 successive detections, the response was still retained 96% of the initial value, suggesting the acceptable operational stability of the proposed biosensor. After a storage period of three weeks in 0.1 M pH 7.0 PBS at 4 °C, the fabricated biosensor showed a 6% loss of the bioactivity. These results indicated that the immobilized GOx retains its high enzymatic activity and the MWCNTs–$SnS_2$ film provided a favorable microenvironment for GOx to perform DET at the modified electrode.

**Table 1**
Comparison of analytical performance between GOx/MWCNTs–$SnS_2$/Nafion/GCE and other modified electrodes.

| Electrode | Applied potential (V) | Sensitivity (mA $M^{-1}$ $cm^{-2}$) | Detection limit (nM) | Linear range (nM) | Reference |
|---|---|---|---|---|---|
| GOx/MWCNTs–$SnS_2$/Nafion/GCE | −0.43 | 21.65 | 0.004 | 0.02–1.95 | This work |
| GOx/$SnS_2$/Nafion/GCE | −0.45 | 7.6 | 0.01 | 0.025–1.1 | Yang et al., 2011 |
| GOx–CNTs-chitosan/GCE | +0.40 | 7.36 | – | 0.0–7.8 | Liu et al., 2005 |
| GOx/CNx–MWNTs | −0.50 | 13.0 | 0.01 | 0.02–1.02 | Deng et al., 2009 |
| Nafion/GOx/Ag-Pdop@CNT/GCE | −0.50 | 3.1 | 0.017 | 0.05–1.1 | Wang et al., 2011 |
| Nafion–CNTs–CdTe-GOx/GCE | – | 14.41 | – | 0.0–0.7 | Liu et al., 2007 |
| Nafion/GOx/PIL-CNTs/GCE | −0.49 | 14.74 | – | 0.05–6.0 | Xiao et al., 2010 |
| Laponite/GOx/GCE | −0.45 | 4.8 | 0.01 | 0.02–1.9 | Shan et al., 2010a, b |
| GOx/Pt/FCNA/GCE | −0.08 | 6.0 | 0.3 | 0.5–8.0 | Tang et al., 2010 |

CNx–MWNTs: nitrogen-doped carbon nanotubes.
Pdop: polydopamine.
PIL: polymerized ionic liquid.
FCNA: flower-like carbon nanosheet aggregation.

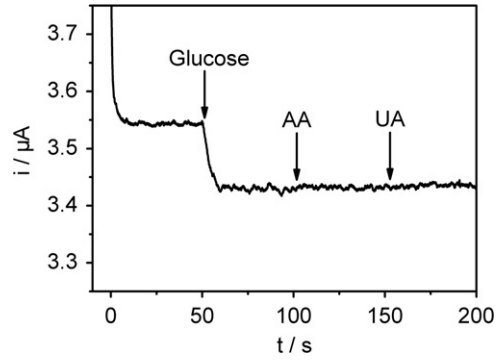


**Fig. 5.** Amperometric response of the GOx/MWCNTs–$SnS_2$/Nafion/GCE to 0.1 mM glucose, 0.1 mM AA and 0.1 mM UA in pH 6.0 PBS at the applied potential of −0.43 V.

### *3.5. Interference study and detection of glucose in the practical serum sample*

The interferences in quantitative electrochemical detection of glucose were examined with 0.1 mM uric acid (UA) and 0.1 mM ascorbic acid (AA) at the applied potential of −0.43 V and shown in Fig. 5. Upon the addition of 0.1 mM glucose to PBS, an obvious current response appeared. After successively injecting the AA and UA into the solution, no obvious increase of the current was observed. These results demonstrated that the proposed biosensor has high selectivity toward glucose in the presence of those endogenously coexisted electroactive substances.

In order to evaluate the practical application of the constructed biosensor, the electrochemical detection of glucose in serum was directly performed without any sample pretreatment except a dilution step. The human serum samples were received from Northern Jiangsu People's Hospital. The glucose level was determined to be 5.46 mM, which is close to the value of 5.65 mM obtained by enzyme catalytic spectrophotometry. The recoveries for the assay of 0.1, 0.2 and 0.3 mM glucose added to the serum samples were 99%, 98% and 102% for five measurements, respectively, indicating good accuracy for the detection of glucose in the real samples.

## 4. Conclusions

A novel MWCNTs wrapped nanoflake-like $SnS_2$ nanocomposite has been proposed for the immobilization of enzyme and glucose biosensing. Compared with single $SnS_2$ or MWCNTs, the resulting nanocomposite has larger specific surface area and provides a more favorable microenvironment for enhancing the electron transfer between the proteins and the electrode surface. The immobilized enzyme on MWCNTs–$SnS_2$ film retains its native structure and bioactivity and exhibits fast amperometric response to glucose. In comparison with our previously fabricated $SnS_2$-based glucose sensor, this constructed glucose biosensor shows more excellent performances such as higher sensitivity (21.65 mA $M^{-1}$ $cm^{-2}$), much lower detection limit (0.004 mM), wider linear range (0.02–1.95 mM) and larger the apparent electron transfer rate constant (3.96 $s^{-1}$). The MWCNTs–$SnS_2$ provides a promising matrix for promoting the direct electron transfer of proteins and developing novel types of biosensors.

## Acknowledgments

This work was financially supported by the National Natural Science Foundation of China (21075107, 21005070, 21275124 and 21103148), The Priority Academic Program Development of Jiangsu Higher Education Institution (PAPD), Postdoctoral Science Foundation of China (20110491462), Postdoctoral Science Foundation of Jiangsu Province (1101020B, 1102142C) and the Open Research Fund of State Key Laboratory of Bioelectronics of Southeast University (2011E13).

## References

Bao, S.J., Li, C., Zang, J.F., Cui, X.Q., Qiao, Y., Guo, J., 2008. Advanced Functional Materials 18, 591–599.
Chu, X.C., Wu, B.H., Xiao, C.H., Zhang, X.H., Chen, J.H., 2010. Electrochimica Acta 55, 2848–2852.
Dai, Z.H., Shao, G.J., Hong, J.M., Bao, J.C., Shen, J., 2009. Biosensors & Bioelectronics 24, 1286–1291.
Deng, C.Y., Chen, J.H., Chen, X.L., Xiao, C.H., Nie, L.H., Yao, S.Z., 2008. Biosensors & Bioelectronics 23, 1272–1277.
Deng, S.Y., Jian, G.Q., Lei, J.P., Hu, Z., Ju, H.X., 2009. Biosensors & Bioelectronics 25, 373–377.
Deshpande, N.G., Sagade, A.A., Gudage, Y.G., Lokhande, C.D., 2007. Journal of Alloys and Compounds 436, 421–426.
Fan, Q., Shan, D., Xue, H.G., He, Y.Y., Cosnier, S., 2007. Biosensors & Bioelectronics 22, 816–821.
Guiseppi-Elie, A., Lei, C., Baughman, R.H., 2002. Nanotechnology 13, 559–564.
Ianniello, R.M., Lindsay, T.J., Yacynych, A.M., 1982. Analytical Chemistry 54, 1098–1101.
Iijima, S., 1991. Nature 354, 56–58.
Jia, F., Shan, C.S., Li, F.H., Niu, L., 2008. Biosensors & Bioelectronics 24, 945–950.
Kang, X.H., Wang, J., Wu, H., Aksay, I.A., Liu, J., Lin, Y.H., 2009. Biosensors & Bioelectronics 25, 901–905.
Kim, T.J., Kim, C., Son, D., Choi, M., Park, B., 2007. Journal of Power Sources 167, 529–535.
Laviron, E., 1979. Journal of Electroanalytical Chemistry 101, 19–28.
Li, F.H., Song, J.X., Li, F., Wang, X.D., Zhang, Q.X., Han, D.X., 2009. Biosensors & Bioelectronics 25, 883–888.
Liu, H.Y., Hu, N.F., 2007. Electroanalysis 19, 884–892.
Liu, Q., Lu, X.B., Li, J., Yao, L., Li, J.H., 2007. Biosensors & Bioelectronics 22, 3203–3209.
Liu, S.Q., Ju, H.X., 2003. Biosensors & Bioelectronics 19, 177–183.

Liu, Y., Wang, M.K., Zhao, F., Hu, Z.A., Dong, S.J., 2005. Biosensors & Bioelectronics 21, 984–988.
Lu, Q., Zhou, T., Hu, S.S., 2007. Biosensors & Bioelectronics 22, 899–904.
Meng, L., Jin, J., Yang, G.X., Lu, T.H., Zhang, H., Cai, C.X., 2009. Analytical Chemistry 81, 7271–7280.
Nadzhafova, O., Etienne, M., Walcarius, A., 2007. Electrochemistry Communications 9, 1189–1195.
Panda, S.K., Antonakos, A., Liarokapis, E., Bhattacharya, S., Chaudhuri, S., 2007. Materials Research Bulletin 42, 576–583.
Pingarron, J.M., Yanez-Sedeno, P., Gonzalez-Cortes, A., 2008. Electrochimica Acta 53, 5848–5866.
Salimi, A., Sharifi, E., Noorbakhsh, A., Soltanian, S., 2007. Biosensors & Bioelectronics 22, 3146–3153.
Seo, J., Jang, J., Park, S., Kim, C., Park, B., Cheon, J., 2008. Advanced Materials 20, 4269–4273.
Shi, C., Liu, Q., Xie, Y., Xu, X., 2003. Journal of Molecular Structure 644, 139–144.
Shan, C.S., Yang, H.F., Han, D.X., Zhang, Q., Ivaska, A., Niu, L., 2010a. Biosensors & Bioelectronics 25, 1070–1074.
Shan, D., Zhang, J., Xue, H.G., Ding, S.N., Cosnier, S., 2010b. Biosensors & Bioelectronics 25, 1427–1433.
Shi, W., Huo, L., Wang, H., Zhang, H., Yang, J., Wei, P., 2006. Nanotechnology 17, 2918–2924.
Tang, S., Wang, X.Z., Lei, J.P., Hu, Z., Deng, S.Y., Ju, H.X., 2010. Biosensors & Bioelectronics 26, 432–436.
Uang, Y., Chou, T.C., 2003. Biosensors & Bioelectronics 20, 2435–2453.
Vamvakai, V., Tsagaraki, K., Chaniotakis, N., 2006. Analytical Chemistry 78, 5538–5542.
Wang, Y.L., Liu, L., Li, M.G., Xu, S.D., Gao, F., 2011. Biosensors & Bioelectronics 30, 107–111.
Wen, D., Liu, Y., Yang, G.C., Dong, S.J., 2007. Electrochimica Acta 52, 5312–5317.
Willner, B., Katz, E., Willner, I., 2006. Current Opinion in Biotechnology 17, 589–596.
Willner, I., Katz, E., 2000. Angewandte Chemie-International Edition 39, 1180–1218.
Wu, S., Ju, X.H., Liu, Y., 2007. Advanced Functional Materials 17, 585–592.
Wu, Y.H., Hu, S.S., 2007. Bioelectrochemistry 70, 335–341.
Xiao, C.H., Chu, X.C., Wu, B.H., Pang, H.L., Zhang, X.H., Chen, J.H., 2010. Talanta 80, 1719–1724.
Xu, X.A., Jiang, S.J., Hu, Z., Liu, S.Q., 2010. ACS Nano 4, 4292–4298.
Yang, C., Wang, W., Shan, Z., Huang, F., 2009. Journal of Solid State Chemistry 182, 807–812.
Yang, Z.J., Huang, X.C., Zhang, Y.C., Li, Juan, Xu, Q., Hu, X.Y., 2012. Electrochimica Acta 70, 325–330.
Yang, Z.J., Ren, Y.Y., Zhang, Y.C., Li, J., Li, H.B., Huang, X.C., Hu, X.Y., Xu, Q., 2011. Biosensors & Bioelectronics 26, 4337–4341.
Yin, H.S., Zhou, Y.L., Meng, X.M., Shang, K., Ai, S.Y., 2011. Biosensors & Bioelectronics 30, 112–117.
Zhang, J.D., Feng, M.L., Tachikawa, H., 2007. Biosensors & Bioelectronics 22, 3036–3041.
Zhang, L.L., Cheng, H.H., Zhang, H.M., Qu, L.T., 2012. Electrochimica Acta 65, 122–126.
Zhang, Y.C., Du, Z.N., Li, S.Y., Zhang, M., 2010. Applied Catalysis B: Environmental 95, 153–159.
Zhao, H.T., Ju, H.X., 2006. Analytical Biochemistry 350, 138–144.
Zheng, H., Xue, H., Zhang, Y., Shen, Z., 2002. Biosensors & Bioelectronics 17, 541–545.